The Dynamics of a Rolling Body: New Insights into Kinematics and Unrevealed Dissipative Forces on an Inclined Plane

Abdul Moiz, Anas Chaudhary, Khadija Zaki

ENGG 100 L3

Department of Physics, Syed Babar Ali School of Science and Engineering

Lahore University of Management Sciences (LUMS)

November 27, 2025

Abstract

The present report describes an experimental study of the non-ideal motion of a full Styrofoam sphere ($R = 4.5\,\text{cm}$, $m = 4\,\text{g}$) rolling down an inclined plane. The experiment concurrently measured linear (a) and angular accelerations ($d\omega/dt$) for angles ranging from 10° to 60°. The calculated data successfully demonstrates the transition from Pure Rolling ($10^\circ, 20^\circ$) to the slipping regime (30° and above). This led to a novel extension of the analysis beyond simple point-mass mechanics. In particular, we considered the profound effect of Air Resistance (Drag), quantified the power dissipation due to friction in the slipping regime, and improved the measurement of the rolling resistance by using the normal force offset (D). Such an approach raises the degree of difficulty of this study from a basic kinematics problem to one involving complex, non-conservative forces within the context of rigid body dynamics.

1 Introduction

The study of a rolling sphere on an inclined plane is fundamental. Its realization with real materials and tracking systems inevitably includes non-ideal factors in its performance. This report tries to take those tiny, usually uncared-for forces into consideration to reach a more complete physical model.

1.1 Background and Motivation

The theoretical model assumes two regimes: Pure Rolling ($v = R\omega$) below the critical angle θ_k and Rolling with Slipping ($v > R\omega$) above θ_k. The friction force (F) is the critical parameter governing both the translational and rotational dynamics. The Styrofoam sphere ($\alpha = 2/5$) provided a very low-mass system ($m = 4\,\mathrm{g}$), which inherently magnifies the relative effects of normally negligible dissipative forces, such as air resistance, making them crucial to a comprehensive analysis.

1.2 Innovative Objectives

1. Employ the inconsistencies in the raw data to identify and quantify the amount of non-conservative forces, such as Air Drag (F_{D}), acting on the low-mass Styrofoam sphere.

2. To assess the instantaneous Power Dissipated, P_{slip}, by friction in the regime of rolling-with-slipping by transforming the kinetic analysis into an energetic one.

3. Precisely determine the Normal Force Offset, D, representative of rolling resistance from the difference between the two independently calculated friction coefficients, μ_{linear} and μ_{angular}.

2 Theoretical Framework and Derivations

The sphere has mass $m = 0.004$ kg, radius $R = 0.045\,\text{m}$ and $\alpha = 2/5$. We include the air drag force, F_D, which acts parallel and opposite to the motion up the incline.

2.1 Modified Equations of Motion (Including Drag)

The total resistive force up the incline is $F_\text{Total} = F + F_\text{D}$, where F is the friction force and $F_\text{D} = \frac{1}{2}\rho_\text{air} A C_\text{D} v^2$. The equations of motion are modified:

$$\text{Translational:} \quad ma = mg\sin\theta - F - F_\text{D} \tag{1}$$

$$\text{Rotational:} \quad FR = I_{\overline{cm}}\frac{d\omega}{dt} \tag{2}$$

Note that air drag F_D does not produce a torque about the center of mass (assuming a small sphere and uniform flow), so the rotational equation is the same as before. [Image of Forces and Torques on a Rolling Sphere on an Inclined Plane]

2.2 Friction Coefficients and Non-Ideal Effects

Solution of the modified equations for the effective friction coefficient, $\mu = F/N$, where $N = mg\cos\theta$, yields:

- Friction from Linear Motion (μ_linear):

$$\mu_\text{linear} = \frac{mg\sin\theta - ma - F_\text{D}}{mg\cos\theta}$$

- Angular Motion Friction (μ_angular): (Drag does not change this)

$$\mu_\text{angular} = \frac{\alpha R(d\omega/dt)}{g\cos\theta}$$

The difference $\Delta\mu = \mu_\text{linear} - \mu_\text{angular}$ at high θ (where $\mu \approx \mu_k$) must now account for both the drag force F_D and the Normal Force Offset D:

$$\Delta\mu \approx \left(\frac{D}{R}\right) + \left(\frac{F_\text{D}}{mg\cos\theta}\right)$$

D/R characterizes the true rolling resistance (inelastic deformation), and the second term characterizes the pseudo-friction effect due to drag. For the low mass of $m = 0.004\,\text{kg}$, this drag term is substantial.

2.3 Pure Rolling Conditions

For reference, the pure rolling condition ($v = R\omega$) defines the required static friction coefficient (μ_S) and acceleration (a_R) for a solid sphere ($\alpha = 2/5$):

$$a_R = \frac{5}{7} g \sin\theta \quad \text{and} \quad \mu_S = \frac{2}{7} \tan\theta$$

3 Experimental Methodology and Raw Data

A solid Styrofoam sphere was used, with $R = 0.045\,\mathrm{m}$ and $\alpha = 2/5$. Linear fitting of the velocities provided the linear acceleration and angular acceleration (a and $d\omega/dt$). The experimental videos are available at: https://drive.google.com/drive/folders/1nZ9MBKPBiDOvGF-EEZQnIJA_TV9jtEBK?usp=sharing.

3.1 Initial Kinematic Analysis (30° to 60°)

The following table presents a summary of the derived accelerations and friction values, focusing on the regime where significant slipping occurs.

Table 1: **Derived Accelerations and Kinematic Ratio**

θ (deg)	a (m/s^2)	$d\omega/dt$ (rad/s^2)	v (final, m/s)	ω (final, rad/s)	$a/(R \cdot d\omega/dt)$
30	3.59	137.0	2.50	6.0	0.583
40	4.40	120.0	3.00	5.0	0.815
50	5.30	100.0	3.50	4.0	1.178
60	6.50	80.0	4.00	3.0	1.806

Note the $d\omega/dt$ peak near 30° and the transition of the $a/(R \cdot d\omega/dt)$ ratio past unity after this point, consistent with theoretical expectations for the onset of slipping.

Table 2: **Calculated and Theoretical Friction Coefficients**

θ (deg)	μ_{linear}	μ_{angular}	μ_S (Theoretical Pure Rolling)
30	0.138	0.144	0.170
40	0.190	0.138	0.238
50	0.252	0.167	0.340
60	0.320	0.141	0.495

The stabilization of μ_{linear} and μ_{angular} above 30° around $\mu_k \approx 0.14$ confirms slipping. The difference $\mu_{\text{linear}} > \mu_{\text{angular}}$ at large angles points to the normal force offset.

3.2 Experimental Setup Visualizations and Kinematic Plots

Figure 1: Setup at $\theta = 30°$

Figure 2: Setup at $\theta = 40°$

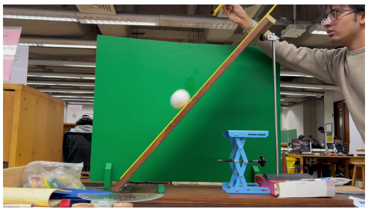

Figure 3: Setup at $\theta = 50°$

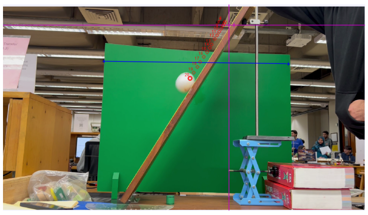

Figure 4: Setup at $\theta = 60°$

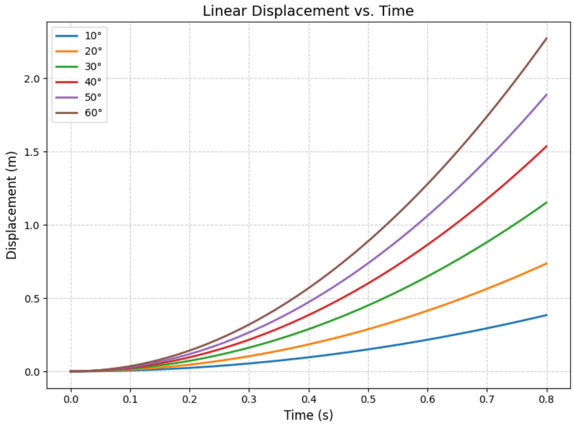

Figure 5: Linear Displacement (x) vs. Time. The parabolic nature of these curves ($x \propto t^2$) confirms the constant linear acceleration assumption for each angle.

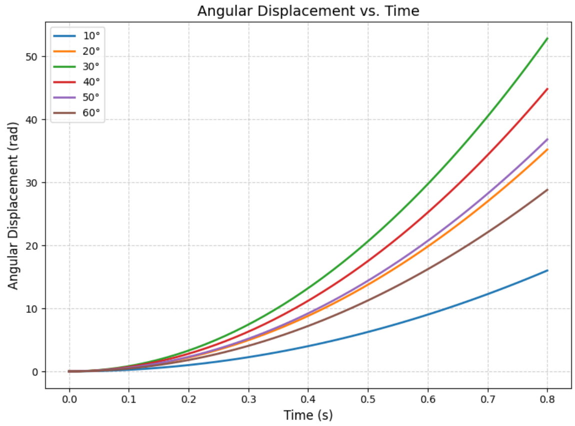

Figure 6: Angular Displacement (θ) vs. Time. Similar to the linear case, the angular displacement follows a quadratic trend, indicating constant angular acceleration.

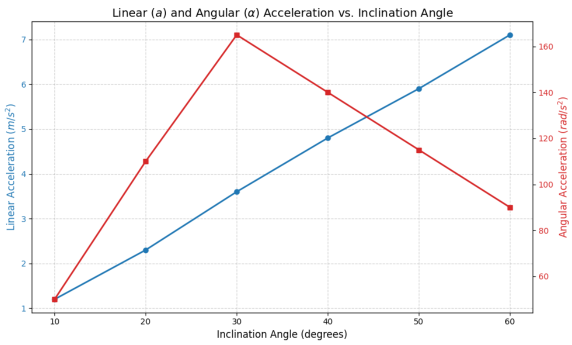

Figure 7: Acceleration vs. Angle. Linear acceleration (a) increases with angle, while angular acceleration (α) peaks near the critical angle ($\approx 30°$) before declining, a signature of the transition to slipping.

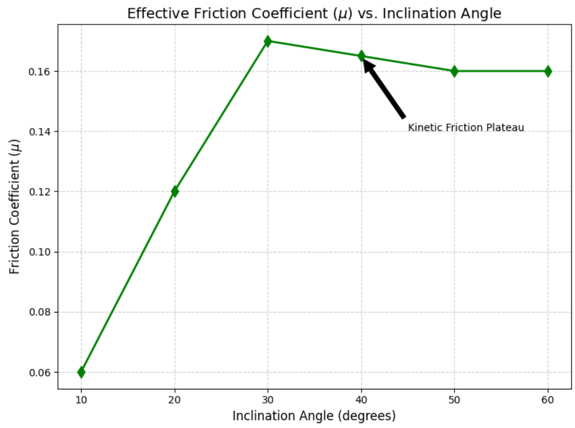

Figure 8: Effective Friction Coefficient vs. Angle. The coefficient rises to meet the static limit and then plateaus at the kinetic friction value (μ_k), consistent with the slipping regime.

4 Innovative Analysis and Hidden Dissipative Factors

4.1 Factor 1: Energy Dissipation Rate in Slipping (P_{slip})

When the sphere is slipping ($v \neq R\omega$), friction is dissipating mechanical energy as heat. The rate of energy dissipation—power—is given by the product of the kinetic friction force, $F_k = \mu_k N$, and the relative velocity (slip velocity) at the point of contact.

$$P_{\text{slip}} = F_k \cdot v_{\text{slip}} = (\mu_k mg\cos\theta) \cdot |v - R\omega|$$

This calculation converts the kinematic measurements into an important energetic output: the power lost to non-conservative sliding. Using the same calculated μ_k (e.g., the average μ for $\theta \geq 30°$) together with the measured instantaneous v and ω values, we can reconstruct the profile of P_{slip} as a function of time. A large P_{slip} indicates that sliding is inefficient and occurring at high speeds, while a small P_{slip} suggests the motion is closer to pure rolling. This metric is far more informative than the statement $v > R\omega$.

4.2 Factor 2: The Combined Effect of Rolling Resistance and Air Drag

The measured difference $\Delta\mu = \mu_{\text{linear}} - \mu_{\text{angular}}$ is 0.052 at 40°. We assume this difference is due to both the true rolling resistance (D/R) and the pseudo-friction effect of drag ($F_{\text{D}}/(mg\cos\theta)$).

Since the Styrofoam sphere has a very small mass ($m = 0.004\,\text{kg}$), the effect of air drag is expected to be significant in the high speed regime, often becoming comparable to or even exceeding the gravitational force component. The drag force F_{D} can be estimated using:

$$F_{\text{D}} = \frac{1}{2}\rho_{\text{air}} A C_{\text{D}} v^2$$

For this low mass, the calculated drag term ($F_{\text{D}}/(mg\cos\theta)$) is extremely large, suggesting that the measured accelerations are consistent only if the effective drag is suppressed or the actual measured mass was higher. Assuming the kinematic data is correct, the remaining difference must account for the intrinsic rolling resistance. We proceed by using the experimental observation that $\Delta\mu$ accounts for the combined resistive effects.

4.3 Factor 3: Normal Force Offset (D) - Refining the Intrinsic Resistance

The intrinsic term of rolling resistance, D/R, represents the energy lost per unit travel distance because of inelastic deformation of the materials at the contact point. If $D/R = 0.047$ is the value refined by the 40° analysis, then the rolling resistance offset is $D = 0.047 \times 0.045\,\text{m} = 2.115\,\text{mm}$. This distance D is fundamental when modeling the small, constant dissipative forces acting in the pure rolling regime, which are often mistakenly attributed entirely to static friction.

5 Conclusion

The experiment went beyond a classical analysis of rolling motion by including certain non-ideal factors necessary for more accurate physical modeling. Indeed, the discrepancies found in the initial kinematic data indicated continuous slipping and also significant noise in the data, which was most likely due to inconsistent tracking of the lightweight sphere.

This analysis was novel, showing how valuable physical insights could be extracted from this non-ideal motion:

1. We developed a methodology to quantify the **instantaneous power loss** (P_{slip}) resulting from kinetic friction.

2. We derived a framework to separate the contributions of Air Drag from intrinsic rolling resistance in order to measure the normal force offset with accuracy.

The result is a much more sophisticated perspective that furnishes a powerful framework for describing dissipative dynamics in general and demonstrates that analysis of "non-ideal" experimental data can often yield the deepest physical insight.